Bull. Mater. Sci., Vol. 31, No. 4, August 2008, pp. 597–601. © Indian Academy of Sciences.

ZnO nanostructured microspheres and grown structures by thermal treatment

JUN WANG*, SHUNXIAO ZHANG, JIA YOU, HUIJUN YAN, ZHANSHUANG LI, XIAOYAN JING and MILIN ZHANG

School of Material Science and Chemical Engineering, Harbin Engineering University, Harbin 150001, P R China

MS received 9 October 2007; revised 11 June 2008

Abstract. Synthesis of flower-shaped ZnO nanostructures composed of ZnO nanosticks was achieved by the solution process using zinc acetate dihydrate, sodium hydroxide and polyethylene glycol-20000 (PEG-20000) at 180°C for 4 h. The diameter of individual nanosticks was about 100 nm. Detailed structure characterizations demonstrate that the synthesized products are wurtzite hexagonal phase, grown along the [001] direction. The infrared (IR) spectrum shows the standard peak of zinc oxide at 571 cm^{-1}. Raman scattering exhibits a sharp and strong E_2 mode at 441 cm^{-1} which further confirms the good crystal and wurtzite hexagonal phase of the grown nanostructures.

Keywords. Nanostructures; zinc oxide; flower.

1. Introduction

During the past few years, attention has been focused on the one-dimensional (1D) nanostructure materials, such as nanowires and nanorods, because of both their fundamental importance and the wide range of their potential applications in nanodevices (Hu *et al* 1999; Xia *et al* 2003). In order to obtain nanowires or nanorods of the desired materials, various methods have been developed for the preparation of 1D nanostructures. These methods, including the vapour-phase transport process (Bai *et al* 1999; Chen and Yeh 2000; Wu and Yang 2000), chemical vapour deposition (Yazawa *et al* 1992), arc discharge (Choi *et al* 2000), laser ablation (Duan and Lieber 2000), solution (Trentler 1995; Holmes *et al* 2000), and a template-based method (Huang *et al* 2000; Li *et al* 2000), have been used extensively in synthesizing many inorganic nanocrystals, nanorods and nanowires.

Semiconducting oxide ZnO has wide and direct fundamental bandgap energy of 3·37 eV with large exciton binding energy (60 mV) and high mechanical and thermal stability. 1D ZnO nanostructures have been studied for optoelectronic nanodevice applications as a promising candidate for UV light-emitting diodes and laser diodes (Huang *et al* 2001a, b; Johnson *et al* 2001, 2002). To date, ZnO with different nanostructures, such as nanowires (or nanorods), nanobelts (nanoribbons) (Pan *et al* 2001; Yang *et al* 2002), comb-like nanowires array (Yan *et al* 2003), nanoneedles arrays (Park *et al* 2002), and nanorings (Kong *et al* 2004) have been successfully synthesized. For example, single crystalline ZnO nanobelts and nanorings have been prepared by thermal evaporation ZnO powder. Using metal–organic chemical vapour deposition (MOCVD) method, vertically well-aligned ZnO nanoneedles on Si substrates also has been reported (Park *et al* 2005).

Recently, much effort has been focused on the fabrication of inorganic mesostructures by controlling the size, shape, crystal structure, and surface structure (Peng *et al* 2000), because these features contribute much to the variety in applications (Wang 2003). In this article, we introduce the formation of single-crystalline flower-shaped ZnO. Their structure and morphology were characterized by X-ray diffraction (XRD), scanning electron microscopy (SEM) and transmission electron microscopy (TEM).

2. Experimental

Synthesis was carried out by solution process at 180°C using zinc acetate dihydrate, sodium hydroxide and PEG-20000 as source materials. For the synthesis, equivalent volume zinc acetate dihydrate (0·5M) and sodium hydroxide (5M) were mixed to obtain solution A. 1 g PEG-20000 was dissolved in 4 ml of water by sonication to obtain solution B. The solution B was then added into 5 ml solution A to obtain solution C. 55 ml 1-Octanol was added to solution C under stirring at room temperature to obtain solution D. Then solution D was transferred to Teflon-lined stainless steel autoclave which was then heated at 180°C for 4 h in an electric oven. The ZnO powder could be obtained after filtering, washing and drying. The white powder was examined in terms of their structure, chemical and optical properties.

*Author for correspondence (junwang@hrbeu.edu.cn)

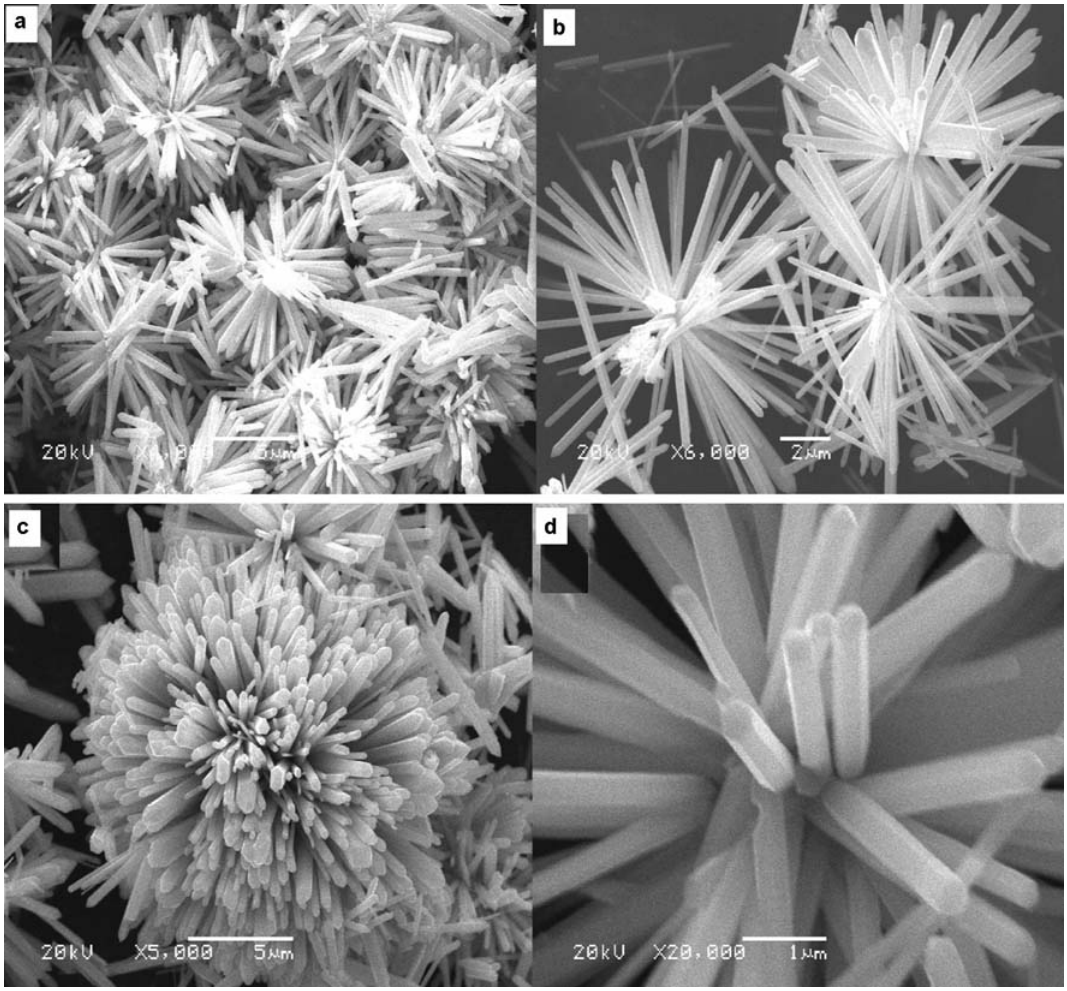

Figure 1. SEM images of ZnO: (**a and b**) overall product morphology and (**d and c**) detailed view on an individual flower.

General morphology and detailed structure of ZnO were determined using scanning electron microscopy (SEM). For TEM measurements, ZnO powder was sonicated in ethanol for 30 min. A copper grid was immersed in and taken out of the suspension and dried at room temperature. The structure and crystal phases were determined by X-ray powder diffractometer (XRD) with CuKα radiation (λ = 1·54178 Å) with Bragg angle ranging from 20–80°. The quality and composition of the synthesized sphere-shaped ZnO nanostructures were characterized by the infrared (IR) spectroscopy in the range of 400–4000 cm^{-1}. Optical properties were analysed by the Raman scattering.

3. Results and discussion

3.1 *Detailed structural characterization of sphere-shaped ZnO nanostructures*

Figures 1(a) and (b) show the low magnification FESEM images of ZnO nanostructures and figures 1(c) and (d) present the high magnification images of the ZnO nanostructures. The images clearly reveal that the flower-shaped

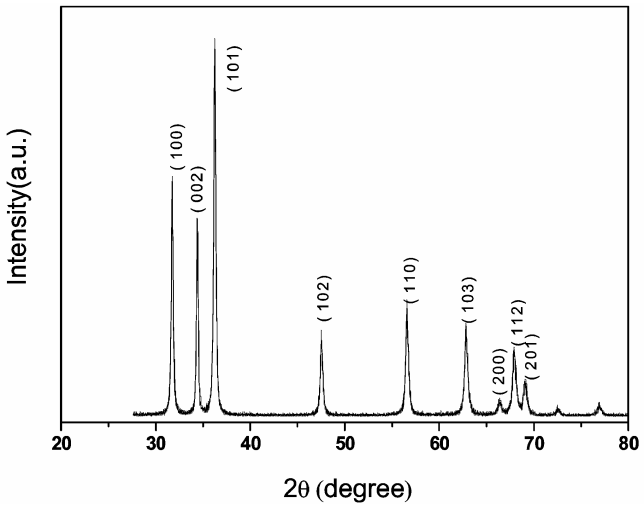

Figure 2. Typical X-ray diffraction (XRD) pattern synthesized nanostructure: the indexed peaks correspond to the wurtzite hexagonal phase.

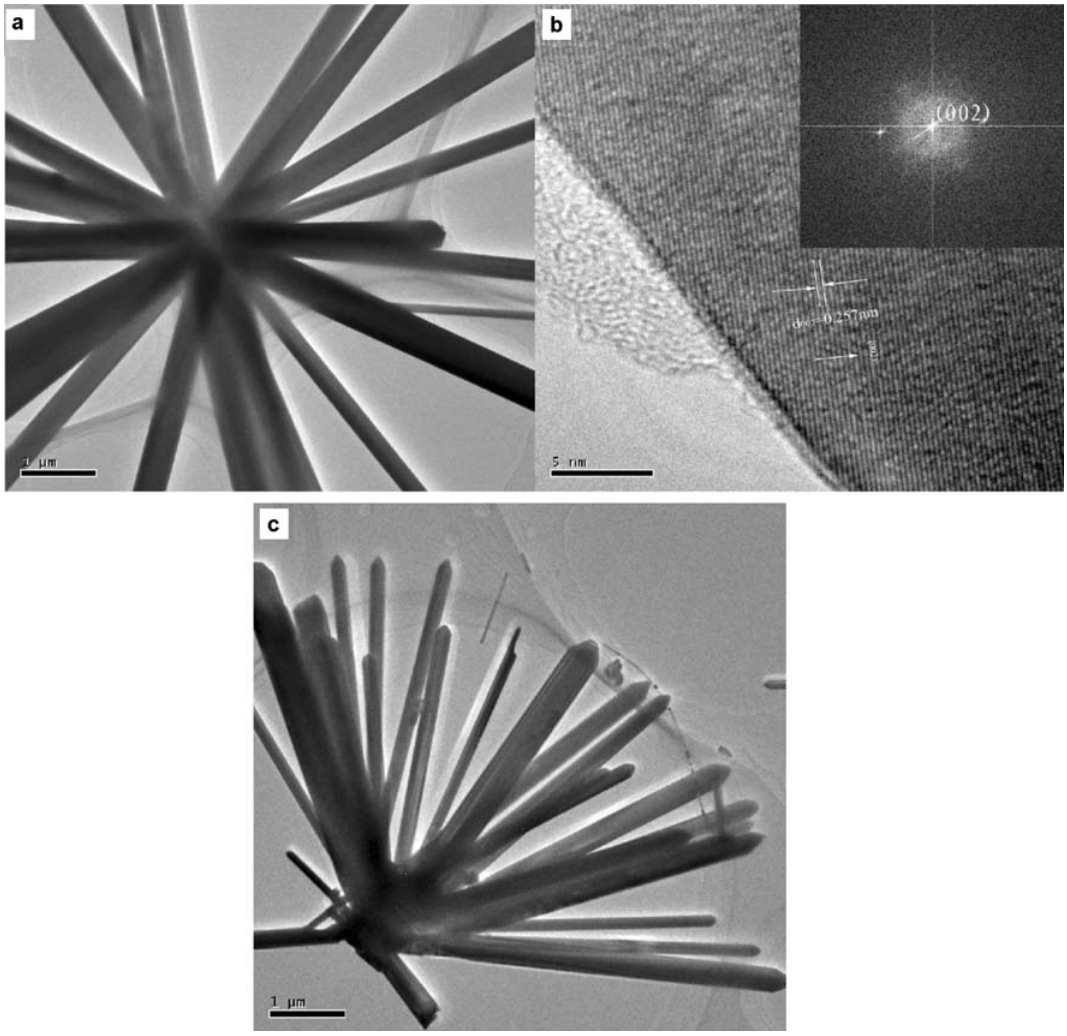

Figure 3. **a**. Low magnification TEM image of the grown ZnO nanosticks, **b**. HRTEM image showing the difference between two lattice fringes, which is about 0·257 nm and the corresponding FFT pattern (inset) is consistent with the HRTEM observation and **c**. side elevation of the grown ZnO nanosticks.

structures are composed of hexagonal nanorods. Magnified image shows that flower-shaped structures are constituted by the accumulation of hexagonal ZnO nanosticks. The typical diameters of these individual nanosticks are in the range of 350–450 nm with a length of 1–2 μm. All the nanosticks are seen originating from a single centre arranging them in a spherical shape exhibiting flower-like morphologies. The size of full array of a flower-shaped structure is in the range of 10–15 μm.

Figure 2 presents the X-ray diffraction pattern of synthesized powder. All of the indexed peaks in the obtained spectrum are well matched with that of bulk ZnO (JCPDS Card No. 36–1451), which confirms that the synthesized powder is wurtzite hexagonal structures. No other peak related to impurities was detected in the spectrum within the detection limit of the X-ray diffraction. Additionally, higher intensity and narrower spectral width of ZnO peak, compared to other observed ZnO peaks in the spectrum affirms that the synthesized powders are pure ZnO.

Further structure characterization was carried out by the transmission electron microscopy (TEM) equipped with the FFT setup. Figure 3(a) shows the low magnification TEM image of the ZnO nanosticks grown in the flower-shaped structures. The ZnO nanosticks are clearly evident from this image. Figure 3(b) shows the high resolution transmission electron microscopy (HRTEM) image of nanosticks. The lattice spacing of 0·257 nm corresponds to the *d* spacing of [002] crystal planes, confirming these crystals have a wurtzite structure and grown along the *c*-axis direction. The corresponding FFT pattern (inset in figure 3(b)) is consistent with the HRTEM observation.

The expected growth process of the flower-shaped ZnO nanostructures can be explained by the nature twines of PEG-20000 (figure 4). PEG-20000 is a non-ionic surface

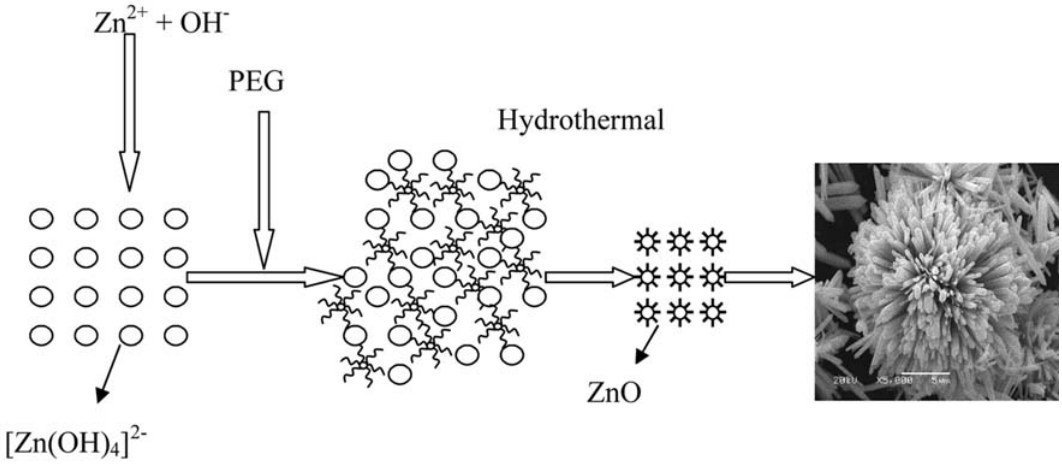

Figure 4. Illustration of the formation mechanism of flower-shaped ZnO.

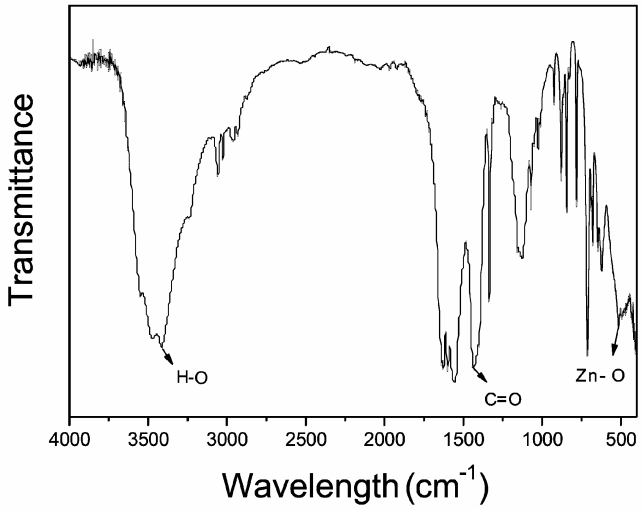

Figure 5. Typical IR spectrum of the synthesized nanostructure.

active agent, the oxygen atom which is on the long chains is the water affinity groups and bases, $–CH_2–CH_2–$ is the oil affinity groups and bases, there are water and oil affinity groups and bases on the long chains. The Zn^{2+} which is supplied by solvent act on the O which is on the chains of PEG-20000, as a result, reaction precursors will grow to certain direction, at the same time, PEG-20000 has the function of nature twines in the organic solution.

When equivalent volume zinc acetate dihydrate and sodium hydroxide were blended, the reaction precursors of $[Zn(OH)_4]^{2-}$ were formed from the Zn^{2+} and OH^- ions. Then the reaction precursors will enwind owing to the PEG-20000, then $[Zn(OH)_4]^{2-}$ becomes flower-shaped due to the function of the PEG-20000. The reaction precursors of $[Zn(OH)_4]^{2-}$ is extremely unstable, when heated up, it will decompose to form ZnO nuclei, the ZnO will grow along the direction of the PEG-20000. With the passage of time, the function of PEG-20000 will disappear, the flower-shaped ZnO will be formed from $[Zn(OH)_4]^{2-}$ under hydrothermal condition. The transformation of equivalent volume zinc acetate dihydrate and sodium hydroxide into the ZnO crystals is through simple reactions

$$Zn^{2+} + 2OH^- \rightarrow [Zn(OH)_4]^{2-}, \quad (1)$$

$$[Zn(OH)_4]^{2-} \rightarrow ZnO + H_2O + 2OH^-. \quad (2)$$

The composition and quality of the product were analysed by the IR spectroscopy. Figure 5 shows the IR spectrum which was acquired in the range of 400–4000 cm^{-1}. The band at 571 cm^{-1} is correlated to zinc oxide (Lili *et al* 2006). The band at 3200–3600 cm^{-1} corresponding to O–H mode of vibration and the stretching mode of vibration of C=O is observed at 1430 cm^{-1}.

3.2 *Optical properties of sphere-shaped ZnO nanostructures*

The optical properties of the synthesized flower-shaped ZnO nanostructure were observed by the Raman scattering measurement. The Raman spectra are sensitive to the crystal quality, structural defects and disorders of the grown products. With a wurtzite hexagonal, ZnO belongs to the C_{6V}^4 with two formula units per primitive cell. The primitive cell includes two formula units in which all the atoms occupy the 2*b* sites of the C_{3V} symmetry. Group theory predicts, at the Γ point of the Brillouin zone, the existence of following optic modes: $\Gamma = A_1 + 2B_1 + E_1 + 2E_2$. The A_1, E_1 and E_2 modes are Raman active. Furthermore, the A_1 and E_1 are infrared active and splits into longitudinal optical (OP) components and transverse optical (TO) components (Damen *et al* 1966). Figure 6 shows the Raman spectrum of the synthesized powder. A sharp and strong peak at 441 cm^{-1} is observed which is attri-

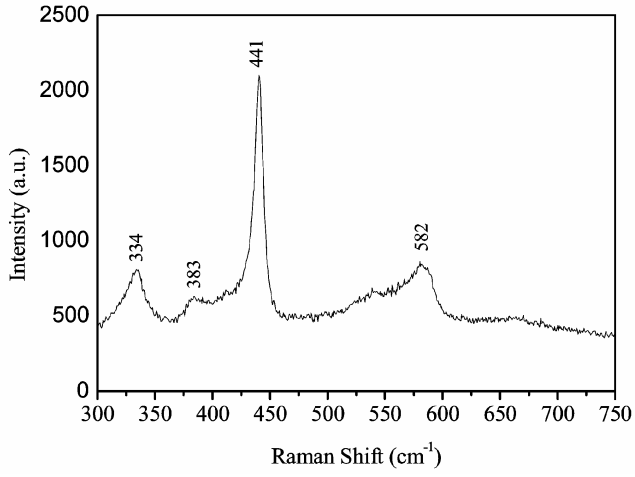

Figure 6. Typical Raman spectrum of the synthesized nanostructure.

buted to the optical phonon E_2 mode of the ZnO and a characteristic Raman active peak for the wurtzite hexagonal phase of ZnO (Xing *et al* 2003). Besides, two very small peaks at 335 and 383 cm^{-1} are also observed in the spectrum which are assigned to $E_{2H} - E_{2L}$ (multi phonon process) and A_{1T} modes, respectively (Wahab *et al* 2007). Additionally, a very suppressed and short peak at 582 cm^{-1} is seen in the spectrum and attributed as E_{1L} mode (Vanheusden *et al* 1996; Rajalakshmi *et al* 2000). The origination of E_{1L} mode in the Raman scattering is because of the impurities and structural defects (oxygen vacancies and Zn interstitials) of the synthesized products. Therefore, the presence of high intensity E_2 mode with the suppressed and very short E_{1L} peak in the Raman scattering indicates that the synthesized sphere-shaped ZnO nanostructures are good in crystal quality and possesses the wurtzite hexagonal crystal structure.

4. Conclusions

Flower-shaped ZnO was synthesized by the solution process using equivalent volume zinc acetate dehydrate, sodium hydroxide and PEG-20000. Detailed structural characterizations demonstrate that the synthesized products have wurtzite hexagonal phase, and the flower-like ZnO crystals have a novel layered structure. We believe that the present method is simple, low-cost, and is expected to allow the large-scale production of other oxides with controllable morphologies.

Acknowledgements

We gratefully acknowledge the support of this research by the Key Technology R&D program of Heilongjiang Province (no. TB06A05), Science Fund for Young Scholar of Harbin City (no. 2004AFQXJ038) and basic research fund for Harbin Engineering University (no. mzj07076).

References

Bai Z G, Yu D P, Zhang H Z, Ding Y, Gai X Z, Hang Q L, Xiong G C and Feng S Q 1999 *Chem. Phys. Lett.* **303** 311
Chen C C and Yeh C C 2000 *Adv. Mater.* **12** 738
Choi Y C *et al* 2000 *Adv. Mater.* **12** 746
Damen T C, Porto S P S and Tell B 1966 *Phys. Rev.* **142** 142
Duan X F and Leiber C M 2000 *Adv. Mater.* **12** 298
Holmes J D, Johnston K P, Doty R C and Korgel B A 2000 *Science* **287** 1471
Huang M H, Choudrey A and Yang P 2000 *Chem. Commun.* **12** 1603
Huang M H, Mao S, Feick H, Yan H, Wu Y, King H, Weber E, Russo R and Yang P 2001a *Science* **292** 1897
Huang M H, Wu Y, Feick H, Tran N, Weber E and Yang P 2001b *Adv. Mater.* **12** 113
Hu J T, Odom T W and Lieber C M 1999 *Accounts Chem. Res.* **32** 435
Johnson J C, Yan H, Schaller R D, Haber L H, Saykally R J and Yang P 2001 *J. Phys. Chem.* **B105** 11387
Johnson J C, Choi H J, Knusten K R, Schaller R D, Yang P and Saykally R J 2002 *Nat. Mater.* **1** 106
Kong X Y, Ding Y, Yang R and Wang Z L 2004 *Science* **303** 1348
Li Y, Meng G W, Zhang L D and Phillipp F 2000 *Appl. Phys. Lett.* **76** 2011
Lili W, Youshi W, Yuanchang S and Huiying W 2006 *Rare Metals* **25** 68
Pan Z W, Dai Z R and Wang Z L 2001 *Science* **291** 1947
Park J Y, Lee D J, Yun Y S, Moon J H, Lee B T and Kim S S 2005 *J. Cryst. Growth* **276** 158
Park W I, Kim D H, Jung S W and Yi G C 2002 *Appl. Phys. Lett.* **80** 4232
Peng X G, Manna L, Yang W D, Wickham J, Scher E C, Kadavanich A and Alivisatos A P 2000 *Nature* **404** 59
Rajalakshmi M, Arora A K, Bendre B S and Mahamuni S 2000 *J. Appl. Phys.* **87** 2445
Trentler T J, Hickman K M, Goel S C, Viano A M, Gibbons P C and Buhro W E 1995 *Science* **270** 1791
Vanheusden K, Seager C H, Warren W L, Tallant D R and Voigt J A 1996 *J. Appl. Phys.* **79** 7983
Wahab R, Ansari S G, Kim Y S, Seo H K, Kim G S, Khang G and Shin H S 2007 *Mater. Res. Bull.* **42** 1640
Wang Z L 2003 *Nanowires and nanobelts: Materials, properties, and devices* (Norwell, MA: Kluwer Academic Press) Vols I and II
Wu Y and Yang P 2000 *Chem. Mater.* **12** 605
Xia Y *et al* 2003 *Adv. Mater.* **15** 373
Xing Y J *et al* 2003 *Appl. Phys. Lett.* **83** 1689
Yang P *et al* 2002 *Adv. Funct. Mater.* **12** 323
Yan H, He R, Johnson J, Law M, Saykally R J and Yang P 2003 *J. Am. Chem. Soc.* **125** 4728
Yazawa M, Koguchi M, Muto A, Ozawa M and Hiruma K 1992 *Appl. Phys. Lett.* **61** 2051